

Spin-incoherent one-dimensional spin-1 Bose Luttinger liquidH. H. Jen¹ and S.-K. Yip^{1,2}¹*Institute of Physics, Academia Sinica, Taipei 11529, Taiwan*²*Institute of Atomic and Molecular Sciences, Academia Sinica, Taipei 10617, Taiwan*

(Received 2 May 2016; published 2 September 2016)

We investigate spin-incoherent Luttinger liquid of a one-dimensional spin-1 Bose gas in a harmonic trap. In this regime highly degenerate spin configurations emerge since the energy splitting between different spin states is much less than the thermal energy of the system, while the temperature is low enough that the lowest energetic orbitals are occupied. As an example we numerically study the momentum distribution of a one-dimensional spin-1 Bose gas in Tonks-Girardeau gas limit and in the sector of zero magnetization. We find that the momentum distributions broaden as the number of atoms increase due to the averaging of spin function overlaps. Large momentum (p) asymptotic is analytically derived, showing the universal $1/p^4$ dependence. We demonstrate that the spin-incoherent Luttinger liquid has a momentum distribution also distinct from spinless bosons at finite temperature.

DOI: [10.1103/PhysRevA.94.033601](https://doi.org/10.1103/PhysRevA.94.033601)**I. INTRODUCTION**

The interacting one-dimensional (1D) quantum system [1] can be described by a low-energy effective theory, so-called Luttinger liquid theory [2]. For spinful systems, one has spin-charge separation but both possess power-law decay of correlation functions. An interesting regime is spin-incoherent Luttinger liquid (SILL) [3] when the temperature is larger than the spin excitation energy while smaller than the charge excitation one. The exponential factor in the single-particle Green's function of SILL puts itself in a different universal class from the Luttinger liquid, and rich physics appears due to the highly degenerate spin Hamiltonian. The semiconductor quantum wire can be a platform to reach SILL regime. In this regime the spin Hamiltonian becomes irrelevant and negligible in the correlation functions that the spin degrees of freedom are nonpropagating [3]. The spin-charge separation still holds simply because the charge velocity is much larger than the spin velocity. In this paper we consider the interacting 1D Bose gas [4] in the spin-incoherent regime. The dispersion relation of the density mode in a spin-1 Bose gas is linear [5], which is the same as the collective charge excitations in the electronic spin-1/2 system. As we will explain later, the spin velocity is much less than the sound velocity; therefore, we also have the spin-incoherent regime if the temperature is higher than the spin excitation energy. We expect that the spin-incoherent 1D Bose gas is even better to demonstrate SILL physics due to the controllability of spatial dimensions and atom-atom interactions.

The strongly interacting and spinless bosonic particles have been experimentally realized in 1D tightly confined systems [6–8]. These hard-core bosons become fermionized in the Tonks-Girardeau (TG) [9,10] gas limit that corresponds to infinitely strong atom-atom interaction, and is one of the few examples that have the exact solutions. In this limit their wave functions can be written down from the constraints that bosons are impenetrable and of bosonic symmetry. In the past two decades many investigations along this line involve the ground-state properties of 1D hard-core bosons [11] and strongly interacting Bose-Fermi mixtures [12] in a harmonic trap, the momentum distribution [13–15], quantum magnetism in 1D

spinor Bose gas [16–20], and using group-theoretical methods in studying the ground states of spin-1/2 fermions [21] and the permutation symmetry of spinor quantum gases [22]. The experimental measurements of such quantum systems rely on the matter wave interferences, for example, the time-of-flight experiment using the focusing technique [23–26], and the Bragg scattering spectroscopy [27–32]. In this paper we investigate the ground-state properties of a 1D spin-1 Bose gas in SILL regime that has not been studied before, and we numerically calculate the momentum distributions that can be observed in experiments. We note that the momentum distributions of spin-1/2 bosons and fermions in SILL regime have been investigated in a homogeneous system [33].

The rest of the paper is organized as follows. In Sec. II we introduce the Hamiltonian of 1D spin-1 Bose gas and the general wave function with spin degree of freedom. In Sec. III, we consider 1D spin-1 Bose gas in TG limit. We derive the general form of density matrix with spin function overlaps assisted by the conjugacy classes of the permutation groups. An analytical derivation of large momentum asymptotic is demonstrated in Sec. IV, and we show the numerically calculated momentum distributions in Sec. V. We conclude in Sec. VI, and the Appendix has the technical details of the traces of various group elements which are used in determining the spin function overlaps.

II. HAMILTONIAN AND WAVE FUNCTION

Starting from the Hamiltonian of ultracold spin-1 Bose gas in one dimension at zero magnetic field [5,16,34],

$$H = \sum_{i=1}^N \left[-\frac{\hbar^2}{2m} \frac{\partial^2}{\partial x_i^2} + \frac{1}{2} m \omega^2 x_i^2 \right] \mathbb{I}_{\text{spin}} + \sum_{i < j} \delta(x_i - x_j) [U_0 \mathbb{I}_{\text{spin}} + U_2 \mathbf{f}_i \cdot \mathbf{f}_j], \quad (1)$$

where \mathbf{f}_i is the spin operator, \mathbb{I}_{spin} is the identity operator in spin space, m is the mass of the bosons, ω is the axial trap frequency, and $U_{0,2}$ are the coupling constants of spin-independent and spin-dependent interactions, respectively. For

a highly elongated trap, the transverse trap frequency (ω_{\perp}) is much larger than ω that the coupling constants effectively are $U_i = 2\hbar\omega_{\perp}c_i$ with $c_0 = (\tilde{a}_0 + 2\tilde{a}_2)/3$, and $c_2 = (\tilde{a}_2 - \tilde{a}_0)/3$, where $\tilde{a}_{0,2} = a_{0,2}/[1 - 1.46a_{0,2}/(\sqrt{2}l_{\perp})]$ [35,36] with s -wave scattering lengths $a_{0,2}$, and $l_{\perp} = \sqrt{\hbar/(m\omega_{\perp})}$ [5]. For ^{23}Na , ^{41}K , and ^{87}Rb , we have $|\tilde{a}_2 - \tilde{a}_0| \ll (\tilde{a}_0 + 2\tilde{a}_2)/3$. For example of ^{87}Rb in the hyperfine state of $F = 1$, $a_0 = 101.8$ and $a_2 = 100.4 a_B$ [37], where a_B is Bohr radius. Therefore, the sound velocity, which is proportional to $\sqrt{c_0}$, is much larger than the spin velocity, which vanishes if $\tilde{a}_2 \approx \tilde{a}_0$.

In TG gas limit of scalar bosons, the system becomes fermionized that bosons do not penetrate each other, and their wave functions take the form of noninteracting fermions. For a spin-1 Bose gas with an infinite atom-atom interaction U_0 in a harmonic trap, we consider a SILL regime [3] where the energy splitting between different spin states is much less than $k_B T$ where k_B is the Boltzmann constant and T is the temperature of the system, while the temperature is low enough that the system still occupies the orbitals in the lowest energy. The regime in general can be reached since $\tilde{a}_2 \approx \tilde{a}_0$ and the difference between them is much less than $(\tilde{a}_0 + 2\tilde{a}_2)/3$.

The wave function in general can be expressed as

$$|\Psi\rangle = \sum_{s_1, s_2, \dots, s_N} \psi_{s_1, s_2, \dots, s_N}(\vec{x}) |s_1, s_2, \dots, s_N\rangle, \quad (2)$$

where $\vec{x} = (x_1, x_2, \dots, x_N)$ denotes the spatial distributions along with the spin configurations of N bosons, that is $|s_1, s_2, \dots, s_N\rangle \equiv |\vec{s}\rangle$. The total wave function must be symmetric under interchange of any two particles. Therefore, it is sufficient to first consider the region of $x_1 < x_2 < \dots < x_N$, and all others can be obtained via symmetry. For the spin part, we consider some degenerate and normalized spin configuration state $|\chi\rangle$. Later we will show that it does not matter which $|\chi\rangle$ we start with. Since TG gas limit suggests null wave functions when x_i approaches x_j , we can construct the symmetrized spatial part of the wave function $|\Psi'\rangle = \psi_{\vec{n}}^{\text{sym}}(\vec{x})|\chi\rangle$ in terms of the eigenfunctions $\phi_{n_j}(x_j)$ of the noninteracting fermions in a harmonic trap as

$$\begin{aligned} \psi_{\vec{n}}^{\text{sym}}(\vec{x}) &= \frac{1}{\sqrt{N!}} \mathbb{A}[\phi_{n_1}(x_1), \phi_{n_2}(x_2), \dots, \phi_{n_N}(x_N)] \\ &\quad \times \text{sgn}(x_2 - x_1) \text{sgn}(x_3 - x_2) \dots \\ &\quad \times \text{sgn}(x_N - x_{N-1}), \end{aligned} \quad (3)$$

where \mathbb{A} is antisymmetrizer (equivalent to a Slater determinant), sgn is the sign function to satisfy the bosonic symmetry, and the factor of $\sqrt{N!}$ guarantees the normalization of the wave function. The eigenfunctions $\phi_n(x)$ [also dimensionless form of $\phi_n(y)$] in a harmonic trap are

$$\phi_n(y) = \frac{1}{\sqrt{2^n n!}} \frac{1}{\pi^{1/4}} H_n(y) e^{-y^2/2}, \quad y \equiv x/x_{ho}, \quad (4)$$

where H_n are Hermite polynomials with the trap frequency ω , the atom mass m , and $x_{ho} \equiv \sqrt{\hbar/(m\omega)}$.

The above can be considered as permutations of the orbitals $\vec{n} = (n_1, n_2, \dots, n_N)$, and note that it should not be mistaken for permutations of \vec{x} for here we have chosen the ordered region $x_1 < x_2 < \dots < x_N$. To access the regions other than $x_1 < x_2 < \dots < x_N$ of the wave function, we can construct them via permutations of the orderings of \vec{x} . There should be a total

of $N!$ regions related to the symmetric group S_N . For $N = 3$ as an example, we have $|\Psi'\rangle$ for the original ordered region, and a permutation of first two particles $P_{12}|\Psi'\rangle = \psi_{\vec{n}}^{\text{sym}}(\vec{x})P_{12}|\chi\rangle$ accesses the spatial region $x_2 < x_1 < x_3$ giving the new spin configuration $P_{12}|\chi\rangle$ for this region. The other four regions can be constructed by permutations of P_{23} , $P_{12}P_{23}$, $P_{23}P_{12}$, and $P_{12}P_{23}P_{12}$ on $|\chi\rangle$. Similar treatments of constructing the wave functions have been used in investigating quantum magnetism [16,17] and magnetic correlations [18] in strongly interacting 1D spinor gases.

Note that the ground-state energy for such N bosons occupying the lowest N orbitals $\vec{n} = (0, 1, \dots, N-1)$ is $E = N^2\hbar\omega/2$. Below we proceed to calculate the density matrix using the wave function we formulate here including the spin degree of freedom.

III. DENSITY MATRIX

Here we provide the formalism to calculate the single-particle density matrix of a spin-1 Bose gas, which reads

$$\rho(x, x') = N \sum_{\vec{s}} \int d\vec{x} \psi_{\vec{s}}^*(x, \vec{x}) \psi_{\vec{s}}(x', \vec{x}), \quad (5)$$

where $\vec{x} = (x_2, x_3, \dots, x_N)$, and a factor of N shows up for the other N possible choices of x and x' . We consider only the region of $x < x'$ which should be symmetric to $x > x'$, and also the ordering of $x_2 < x_3 < \dots < x_N$. For $N = 3$ as an example we have the spin function overlaps in $\rho(x, x')$, for a given choice of $|\chi\rangle$,

$$\begin{aligned} x < x_2 < x_3, \quad x' < x_2 < x_3, \quad \langle \chi | E | \chi \rangle &= 1, \\ x_2 < x' < x_3, \quad \langle \chi | P_{12} | \chi \rangle, \\ x_2 < x_3 < x', \quad \langle \chi | P_{23} P_{12} | \chi \rangle, \\ x_2 < x < x_3, \quad x_2 < x' < x_3, \quad \langle \chi | E | \chi \rangle &= 1, \\ x_2 < x_3 < x', \quad \langle \chi | P_{12}^{-1} P_{23} P_{12} | \chi \rangle, \\ x_2 < x_3 < x, \quad x_2 < x_3 < x', \quad \langle \chi | E | \chi \rangle &= 1, \end{aligned} \quad (6)$$

where the first two columns represent the integral regions of x and x' , and the third column is the spin function overlap in this region. E is the identical permutation operator, and we note that $P_{12}^{-1}P_{23}P_{12} = P_{13}$ and $P_{23}P_{12} = P_{123}$. After averaging over a set of spin states $|\chi\rangle$ (to be specified below), we then have the single-particle density matrix,

$$\begin{aligned} \rho(x < x') &= 3 \times 2 \times \left\{ \int_{x < x' < x_2 < x_3} 1 \right. \\ &\quad + \int_{x < x_2 < x' < x_3} \frac{\text{Tr}_{\chi}(P_{12})}{\text{Tr}_{\chi}(E)} \\ &\quad + \int_{x < x_2 < x_3 < x'} \frac{\text{Tr}_{\chi}(P_{123})}{\text{Tr}_{\chi}(E)} + \int_{x_2 < x < x' < x_3} 1 \\ &\quad \left. + \int_{x_2 < x < x_3 < x'} \frac{\text{Tr}_{\chi}(P_{13})}{\text{Tr}_{\chi}(E)} + \int_{x_2 < x_3 < x < x'} 1 \right\} \\ &\quad \times \psi_{\vec{n}}^{\text{sym}*}(x, x_2, x_3) \psi_{\vec{n}}^{\text{sym}}(x', x_2, x_3) dx_2 dx_3, \end{aligned} \quad (7)$$

where the multiplication factor of 2 in the above is due to the contribution of the integral region $x_2 > x_3$. This region can be assessed by interchanging x_2 and x_3 using P_{23} , where the spin function overlaps are equivalent to those with $x_2 < x_3$. The trace (Tr) of the permutation operator over $|\chi\rangle$ is just the summation of the spin function overlaps over all spin configurations, that is $\text{Tr}_\chi(P_{ij\dots k}) = \sum_\chi \langle \chi | P_{ij\dots k} | \chi \rangle$. To account for all the spin configurations, we have made an average over all the spin function overlaps in each integral with the total number of states given by $\text{Tr}_\chi(E)$ since $\langle \chi | E | \chi \rangle = 1$.

To proceed and from now on we shall limit ourselves to the specific sector of total $S_z \equiv \sum_{i=1}^N \langle \hat{S}_z^i \rangle = 0$, where \hat{S}_z^i is z -component spin operator for i th particle. Then we have two possible sets of spin configurations, $\{|\chi_1\rangle^P\} = |000\rangle$, and $\{|\chi_2\rangle^P\} = |+-0\rangle, |-+0\rangle, |0+-\rangle, |0-+\rangle$, composing of six permuted states, which make up of seven states in total. We denote $(-, 0, +)$ as three quantum numbers $(-1, 0, 1)$ for a spin-1 boson, and the superscript P for a permuted set of spin configurations. Then the density matrix becomes

$$\rho(x < x') = 3 \times 2 \times \left\{ \int_{x < x' < x_2 < x_3} 1 + \int_{x < x_2 < x' < x_3} \frac{1}{7} + \int_{x < x_2 < x_3 < x'} \frac{1}{7} + \int_{x_2 < x < x' < x_3} 1 + \int_{x_2 < x < x_3 < x'} \frac{1}{7} + \int_{x_2 < x_3 < x < x'} 1 \right\} \psi_n^{sym*}(x, x_2, x_3) \psi_n^{sym}(x', x_2, x_3) dx_2 dx_3, \tag{8}$$

where we note that $\text{Tr}_\chi(P_{12}) = \text{Tr}_\chi(P_{13})$. The permutations of P_{12} , P_{13} , and P_{23} are conjugate with each other to form a conjugacy class [38]; therefore, they have the same trace. In the S_3 permutation group, E , P_{12} , and P_{123} belong to three different classes. Their traces can be explicitly done and they are also listed in the Appendix.

In general for $x < x'$, we have

$$\rho(x < x') = N! \left\{ \int_{x < x' < x_2 \dots < x_N} 1 + \int_{x < x_2 < x' \dots < x_N} \frac{w_{2N}}{w_N} + \int_{x < x_2 < x_3 < x' \dots < x_N} \frac{w_{3N}}{w_N} + \dots + \int_{x_2 < x < x' \dots < x_N} 1 + \int_{x_2 < x < x_3 < x' \dots < x_N} \frac{w_{2N}}{w_N} + \dots + \int_{x_2 < x_3 \dots < x_N < x < x'} 1 \right\} \psi_n^{sym*}(x, \bar{x}) \psi_n^{sym}(x', \bar{x}) d\bar{x}, \tag{9}$$

where the averaged spin function overlaps are given by $\frac{w_{jN}}{w_N}$, with

$$w_{jN} \equiv \text{Tr}_\chi(P_{12\dots j}), \tag{10}$$

the trace of $P_{12\dots j}$, averaged by

$$w_N \equiv \text{Tr}_\chi(E), \tag{11}$$

the total number of states $|\chi\rangle$. The spin function overlaps can be calculated using the conjugacy class G of symmetric group S_N where we demonstrate up to $N = 6$ in the Appendix. In addition the identity relation of $\sum_G \text{Tr}_\chi G = N!$, the order of S_N , is useful to check on the calculation of various spin function overlaps. Note that the integral regions of permuted \bar{x} are identical; therefore, the density matrix $\rho(x < x')$ has $N(N + 1)/2$ distinguished ones.

Here we show how we calculate the general spin function overlaps in the sector of $S_z = 0$. The spin configurations $\{|\chi_i\rangle^P\}$ in general involves $|00\dots 0\rangle$ and n pairs of $(+-)$, that is $|++\dots -0\dots 0\rangle$ with $n = 2$ for example. For $\{|\chi_i\rangle^P\} = |00\dots 0\rangle$, the trace of any permutation operator is 1. For the spin configuration of n pairs of $(+-)$, the trace of $P_{12\dots j}$ has three contributions. One contribution is that the first j entries are (0) 's, where the spin configuration can be shown as

$$| \underbrace{00\dots 0}_j \underbrace{00\dots 0}_{N-2n-j} \underbrace{+\dots +}_n \underbrace{-\dots -}_n \rangle.$$

The trace is $(N - j)! / [(n!)^2 (N - 2n - j)!]$ since this is the number of states obtained by permuting the rest of $(N - 2n - j)$ (0) 's and n $(+)$'s and $(-)$'s. The other two contributions are for j $(+)$'s or $(-)$'s, which is $(N - j)! / [(n - j)! n! (N - 2n)!]$, the number of states obtained by permuting the rest of $(n - j)$

$(+)$'s or $(-)$'s, n $(-)$'s or $(+)$'s, and $(N - 2n)$ (0) 's. In general, we have the traces for the conjugacy classes of $P_{12\dots j}$ as

$$w_{jN} \equiv \sum_{n=0}^{\frac{N}{2} \text{ or } \frac{N-1}{2}} \left[\frac{(N - j)!}{(n!)^2 (N - 2n - j)!} + \frac{2(N - j)!}{(n - j)! n! (N - 2n)!} \right], \tag{12}$$

for even or odd N with the upper limit of summation as $N/2$ or $(N - 1)/2$, respectively. We note that all the arguments of the factorials should be equal and larger than zero. The total number of states is then calculated as

$$w_N \equiv \sum_{n=0}^{\frac{N}{2} \text{ or } \frac{N-1}{2}} \frac{N!}{(n!)^2 (N - 2n)!}. \tag{13}$$

The spin function overlaps are identical if the permutations are in the same conjugacy class of S_N . The values of w_{jN} can be found in the Appendix.

The momentum distributions of 1D Bose gas in TG limit is then numerically integrated based on Eq. (9) which we will demonstrate in Sec. V. The definition of the momentum distribution is

$$\rho(p) = \frac{1}{2\pi} \int_{-\infty}^{\infty} dx \int_{-\infty}^{\infty} dx' e^{ip(x-x')} \rho(x, x'), \tag{14}$$

where we let $\hbar = 1$. Next we are interested in deriving the asymptotic forms in large momentum limit, which show $1/p^4$ decay and can be measured in experiments.

IV. LARGE p EXPANSION IN $\rho(p)$

Here we show the analytical result of a large p asymptotic in the one-body momentum distribution of 1D TG Bose gas. It is well known that this large asymptotic shall show the universal $1/p^4$ dependence for a Bose gas with two-body contact interactions [13–15]. This universal asymptotic has recently drawn a lot of attention in deriving the energetics (so-called Tan’s relation) [39] and universal properties of the two-component Fermi gas [40–43], and in extending Tan’s relations in one dimension [44]. Before we present the general expression of the large p asymptotic for arbitrary N , we show the results of $N = 2$ and 3 for demonstration.

A. $N = 2$

We first recall of $\rho(x < x')$ for two bosons in Eq. (9) that

$$\rho(x < x') = 2! \left[\int_{x < x' < x_2} 1 + \int_{x < x_2 < x'} \frac{w_{22}}{w_2} + \int_{x_2 < x < x'} 1 \right] dx_2 \psi_n^{sym*}(x, x_2) \psi_n^{sym}(x', x_2). \quad (15)$$

If we replace the coefficient from the averaged spin function overlap ($w_{22}/w_2 = 1/3$) by (-1) , we end up with $\rho(x, x')$ equivalent to the results of the noninteracting fermions, therefore $\rho(p) \propto e^{-(px_{ho})^2}$. Subtracting this vanishing part of $e^{-(px_{ho})^2}$ in large p limit, we have

$$\begin{aligned} \rho(p) &\underset{p \rightarrow \infty}{=} \frac{2!}{2\pi} \int_{-\infty}^{\infty} dx dx' e^{ip(x-x')} \int_{x < x_2 < x'} dx_2 \left(\frac{w_{22}}{w_2} + 1 \right) \psi_n^{sym*}(x, x_2) \psi_n^{sym}(x', x_2) + (x' < x), \\ &\underset{p \rightarrow \infty}{=} \frac{1}{2\pi} \int_{-\infty}^{\infty} dx dx' e^{ip(x-x')} \left[-\frac{4}{3} \int_{x < x_2 < x'} dx_2 \right] \begin{vmatrix} \phi_0(x) & \phi_1(x) \\ \phi_0(x_2) & \phi_1(x_2) \end{vmatrix} \begin{vmatrix} \phi_0(x') & \phi_1(x') \\ \phi_0(x_2) & \phi_1(x_2) \end{vmatrix} + (x' < x), \end{aligned} \quad (16)$$

where we have used Eq. (3), and the second term represents the part of integrals for $x' < x$.

Letting $\bar{y} = x - x_2$ and $\bar{y}' = x' - x_2$ with $d\bar{y} = dx$ and $d\bar{y}' = dx'$, we have

$$\rho(p) \underset{p \rightarrow \infty}{=} \frac{1}{2\pi} \frac{-4}{3} \left[\int_{-\infty}^0 d\bar{y} \int_0^{\infty} d\bar{y}' + \int_{-\infty}^0 d\bar{y}' \int_0^{\infty} d\bar{y} \right] e^{ip(\bar{y}-\bar{y}')} \int_{-\infty}^{\infty} dx_2 \begin{vmatrix} \phi_0(\bar{y} + x_2) & \phi_1(\bar{y} + x_2) \\ \phi_0(x_2) & \phi_1(x_2) \end{vmatrix} \begin{vmatrix} \phi_0(\bar{y}' + x_2) & \phi_1(\bar{y}' + x_2) \\ \phi_0(x_2) & \phi_1(x_2) \end{vmatrix}. \quad (17)$$

Since p is large, \bar{y} and \bar{y}' are necessarily small so we can expand the determinants by Taylor expansion. Also since the zeroth-order expansion gives null results, we keep the nonvanishing first-order expansion, which are the order of \bar{y} and \bar{y}' in the integrals. We then have

$$\begin{aligned} \rho(p) &\underset{p \rightarrow \infty}{=} \frac{1}{2\pi} \frac{-4}{3} \left[\int_{-\infty}^0 d\bar{y} \int_0^{\infty} d\bar{y}' + \int_{-\infty}^0 d\bar{y}' \int_0^{\infty} d\bar{y} \right] \\ &\times \bar{y} \bar{y}' e^{ip(\bar{y}-\bar{y}')} \int_{-\infty}^{\infty} dx_2 \begin{vmatrix} \phi'_0(x_2) & \phi'_1(x_2) \\ \phi_0(x_2) & \phi_1(x_2) \end{vmatrix}^2, \end{aligned} \quad (18)$$

where the prime on the eigenfunctions means the derivative.

We then proceed to solve the above integrals by the integration by parts. For brevity we just demonstrate the integrals of \bar{y} and \bar{y}' ,

$$\int_{-\infty}^0 d\bar{y} \int_0^{\infty} d\bar{y}' e^{ip(\bar{y}-\bar{y}')} \bar{y} \bar{y}' = \frac{-1}{p^4}, \quad (19)$$

where we have imposed the conditions of negligible contribution at the infinite boundary. Note that the part of $(\bar{y} \leftrightarrow \bar{y}')$ gives the same result and putting the above back to $\rho(p)$, we have

$$\begin{aligned} \rho(p) &\underset{p \rightarrow \infty}{=} \frac{4/3}{2\pi} \frac{2}{p^4} \int_{-\infty}^{\infty} dx_2 \begin{vmatrix} \phi'_0(x_2) & \phi'_1(x_2) \\ \phi_0(x_2) & \phi_1(x_2) \end{vmatrix}^2 \\ &= \frac{4/3}{2\pi} \frac{2}{p^4} \int_{-\infty}^{\infty} \frac{e^{-2y^2} dy}{\pi(x_{ho})^3} \begin{vmatrix} -y & \sqrt{2}(1-y^2) \\ 1 & \sqrt{2}y \end{vmatrix}^2, \end{aligned} \quad (20)$$

where we substitute x_2 by $y = x_2/x_{ho}$ in ϕ_n . Further we use the dimensionless $\hbar\bar{k} = \bar{p}$ replacing of $p/\sqrt{m\hbar\omega}$, and we have

$$\begin{aligned} \frac{\rho(\bar{k})}{x_{ho}} &\underset{\bar{k} \rightarrow \infty}{=} \frac{4/3}{2\pi} \frac{2}{\bar{k}^4} \int_{-\infty}^{\infty} \frac{2e^{-2y^2} dy}{\pi}, \\ &= \frac{4/3}{2\pi} \frac{2}{\bar{k}^4} \frac{2}{\pi} \sqrt{\frac{\pi}{2}} = \frac{0.34}{\bar{k}^4}. \end{aligned} \quad (21)$$

B. $N = 3$

Toward the general expression of large p asymptotic for arbitrary N , we show one more example of three bosons. Recalling again Eq. (9), we have six integral regions in $\rho(x < x')$,

$$\begin{aligned} 3! &\left[\int_{x < x' < x_2 < x_3} 1 + \int_{x < x_2 < x' < x_3} \frac{w_{23}}{w_3} + \int_{x < x_2 < x_3 < x'} \frac{w_{33}}{w_3} \right. \\ &\left. + \int_{x_2 < x < x' < x_3} 1 + \int_{x_2 < x < x_3 < x'} \frac{w_{23}}{w_3} + \int_{x_2 < x_3 < x < x'} 1 \right] \\ &\times dx_2 dx_3 \psi_n^{sym*}(x, x_2, x_3) \psi_n^{sym}(x', x_2, x_3), \end{aligned} \quad (22)$$

where $w_{23}/w_3 = w_{33}/w_3 = 1/7$. We can again subtract from the above the corresponding expression of the Fermi gas, which has only $e^{-(px_{ho})^2}$ contribution in the large p limit. Further, noting again that $\rho(p)$ has significant contributions only from the regions of $x < x_j < x'$ and $x' < x_j < x$ for all

$x_j \in \bar{x}$, we then have the remaining terms only from $w_{23}/w_3 \rightarrow w_{23}/w_3 + 1$ in Eq. (22) for $p \rightarrow \infty$,

$$\rho(p) \underset{p \rightarrow \infty}{=} \frac{1}{2\pi} \int_{-\infty}^{\infty} dx dx' e^{ip(x-x')} \left[-\frac{8}{7} \int_{x < x_2 < x' < x_3} -\frac{8}{7} \int_{x_2 < x < x_3 < x'} \right] dx_2 dx_3 \times \begin{vmatrix} \phi_0(x) & \phi_1(x) & \phi_2(x) \\ \phi_0(x_2) & \phi_1(x_2) & \phi_2(x_2) \\ \phi_0(x_3) & \phi_1(x_3) & \phi_2(x_3) \end{vmatrix} \begin{vmatrix} \phi_0(x') & \phi_1(x') & \phi_2(x') \\ \phi_0(x_2) & \phi_1(x_2) & \phi_2(x_2) \\ \phi_0(x_3) & \phi_1(x_3) & \phi_2(x_3) \end{vmatrix} + (x' < x). \quad (23)$$

Again we change variables by $\bar{y} = x - x_2$, $\bar{y}' = x' - x_2$, or $x_2 \rightarrow x_3$. Similar to the derivation of $N = 2$, we expand the above to the first order of \bar{y} and \bar{y}' , apply Eq. (19), and we have

$$\rho(p) \underset{p \rightarrow \infty}{=} \frac{1}{2\pi} \frac{8}{7} \frac{2}{p^4} \int_{-\infty}^{\infty} dx_2 dx_3 \Big|_{x_2 < x_3} \left[\begin{vmatrix} \phi'_0(x_2) & \phi'_1(x_2) & \phi'_2(x_2) \\ \phi_0(x_2) & \phi_1(x_2) & \phi_2(x_2) \\ \phi_0(x_3) & \phi_1(x_3) & \phi_2(x_3) \end{vmatrix}^2 + \begin{vmatrix} \phi'_0(x_3) & \phi'_1(x_3) & \phi'_2(x_3) \\ \phi_0(x_2) & \phi_1(x_2) & \phi_2(x_2) \\ \phi_0(x_3) & \phi_1(x_3) & \phi_2(x_3) \end{vmatrix}^2 \right]. \quad (24)$$

The two terms inside the bracket are equivalent via $x_2 \leftrightarrow x_3$; therefore, we can combine these two terms, but now we can integrate over all x_2 and x_3 . We then expand the determinant into minors, and integrate out either x_2 or x_3 , obtaining

$$\rho(p) \underset{p \rightarrow \infty}{=} \frac{1}{2\pi} \frac{8}{7} \frac{2}{p^4} \int_{-\infty}^{\infty} dx \left[\begin{vmatrix} \phi'_1(x) & \phi'_2(x) \\ \phi_1(x) & \phi_2(x) \end{vmatrix}^2 + \begin{vmatrix} \phi'_0(x) & \phi'_2(x) \\ \phi_0(x) & \phi_2(x) \end{vmatrix}^2 + \begin{vmatrix} \phi'_0(x) & \phi'_1(x) \\ \phi_0(x) & \phi_1(x) \end{vmatrix}^2 \right]. \quad (25)$$

From the above, it suggests that the integrals involve the determinants with a combination of every two eigenfunctions. To proceed, we put in the Hermite polynomials, and use the dimensionless \bar{k} ,

$$\frac{\rho(\bar{k})}{x_{ho}} \underset{\bar{k} \rightarrow \infty}{=} \frac{2 \times 8/7}{2\pi \bar{k}^4} \frac{1}{\pi} \int_{-\infty}^{\infty} dy e^{-2y^2} \left[2 + \begin{vmatrix} -y & \frac{5y-2y^3}{\sqrt{2}} \\ 1 & \frac{2y^2-1}{\sqrt{2}} \end{vmatrix}^2 + \begin{vmatrix} \sqrt{2}(1-y^2) & \frac{5y-2y^3}{\sqrt{2}} \\ \sqrt{2}y & \frac{2y^2-1}{\sqrt{2}} \end{vmatrix}^2 \right] = \frac{2 \times 8/7}{2\pi \bar{k}^4} \frac{27\sqrt{\pi/2}}{4\pi} = \frac{0.98}{\bar{k}^4}. \quad (26)$$

C. General large p asymptotic

In general for arbitrary N , we have

$$\frac{\rho(p)}{N} \underset{p \rightarrow \infty}{=} \frac{(N-1)!}{N!} \frac{2[1 + w_{2N}/w_N]}{2\pi p^4} \sum_{j=2,3,\dots,N} \int_{x_2 < x_3 < \dots < x_N} d\bar{x} \begin{vmatrix} \phi'_{n_1}(x_j) & \phi'_{n_2}(x_j) & \dots \\ \phi_{n_1}(x_j) & \phi_{n_2}(x_j) & \dots \\ \vdots & \dots & \vdots \\ \phi_{n_1}(x_N) & \dots & \phi_{n_N}(x_N) \end{vmatrix}^2, \quad (27)$$

where the factor of $(N-1)!$ is from the permutation of the ordering $x_2 < x_3 \dots < x_N$. The above derivation of Eq. (27) simply generalizes the previous case of $N = 3$. We have expanded the determinants by Taylor expansion for $x \approx x_j \approx x'$, and used Eq. (19) for the Fourier transform. We have also rearranged the rows of the above determinant. Absorbing the factor of $(N-1)!$ to form all space integrals in \bar{x} , we have

$$\rho(p) \underset{p \rightarrow \infty}{=} \frac{1}{(N-1)!} \frac{2[1 + w_{2N}/w_N]}{2\pi p^4} \sum_{j=2,3,\dots,N} \int_{-\infty}^{\infty} d\bar{x} \times \begin{vmatrix} \phi'_{n_1}(x_j) & \phi'_{n_2}(x_j) & \dots \\ \phi_{n_1}(x_j) & \phi_{n_2}(x_j) & \dots \\ \vdots & \dots & \vdots \\ \phi_{n_1}(x_N) & \dots & \phi_{n_N}(x_N) \end{vmatrix}^2. \quad (28)$$

From the orthogonality of the eigenfunctions ϕ_n , finally we can reduce the above as

$$\rho(p) \underset{p \rightarrow \infty}{=} \frac{2[1 + \frac{w_{2N}}{w_N}]}{2\pi p^4} \sum_{(n_i, n_j)} \int_{-\infty}^{\infty} dx \begin{vmatrix} \phi'_{n_i}(x) & \phi'_{n_j}(x) \\ \phi_{n_i}(x) & \phi_{n_j}(x) \end{vmatrix}^2, \quad (29)$$

where (n_i, n_j) denotes any possible pairs of N eigenfunctions, and the factor $(N-1)!$ cancels out by $(N-1)$ summations of x_j within each there are $(N-2)!$ copies of the minors. In the below we show specifically the results for finite number of atoms up to $N = 6$.

For $N = 4$, we have 10 terms of integral regions. From Eq. (29), we have

$$\frac{\rho(\bar{k})}{x_{ho}} \underset{\bar{k} \rightarrow \infty}{=} \frac{2 \times 24/19}{2\pi \bar{k}^4} \frac{18.604}{\pi} = \frac{2.38}{\bar{k}^4}. \quad (30)$$

For $N = 5$ and 6 , we have respectively

$$\frac{\rho(\bar{k})}{x_{ho}} \Big|_{\bar{k} \rightarrow \infty} = \frac{2 \times 64/51}{2\pi \bar{k}^4} \frac{33.57}{\pi} = \frac{4.27}{\bar{k}^4}, \quad (31)$$

$$\frac{\rho(\bar{k})}{x_{ho}} \Big|_{\bar{k} \rightarrow \infty} = \frac{2 \times 180/141}{2\pi \bar{k}^4} \frac{53.93}{\pi} = \frac{6.98}{\bar{k}^4}. \quad (32)$$

The above factors of $24/19$, $64/51$, and $180/141$ for $N=4-6$ respectively are equal to $1 + w_{2N}/w_N$. Equations (30)–(32) are exactly the forms that follow Eq. (29). The factors $18.604/\pi$, $33.57/\pi$, and $53.93/\pi$ are the sums over (n_i, n_j) in Eq. (29) where we obtain the integrals of the determinants numerically.

V. NUMERICAL RESULTS AND DISCUSSIONS

The momentum distribution of a 1D spinor Bose gas has been studied in some selected spin configurations [16], which shows Friedel-like oscillations similar to the noninteracting fermions or broadened momentum distributions depending on the symmetry of the spin functions. Here we consider the spin-incoherent regime using Eq. (9), and demonstrate the momentum distribution of a 1D spin-1 Bose gas in TG limit. We use the Monte Carlo (MC) integration method to derive $\rho(x, x')$, which is implemented in Linux system with message processing interface. To have a sense of the computation time, for $N = 5$ with MC simulations of $M = 1 \times 10^7$ sets of random numbers, it requires about two days with 250 parallel CPU cores.

In Fig. 1, the momentum distribution is demonstrated up to $N = 6$. As the number of particles increases, its momentum distribution broadens almost uniformly in the peaks and the widths. This hugely contrasts with noninteracting fermions or spinless bosons, which have Friedel oscillations or narrower peaks at $p = 0$, respectively. The uniformly broadened and structureless distribution is due to the spin function overlaps in the spin-incoherent regime that averages out the oscillatory features. The MC simulations in Fig. 1 are $M = 1 \times 10^4$, 1×10^5 , 1×10^6 , 1.8×10^8 , and 3.5×10^8 for $N = 2-6$. In contrast, the results of spinless bosons (or equivalently fully spin polarized) are shown in Fig. 2, where we have a sharp momentum distribution as N increases, while the widths of the distributions stay almost the same. Therefore, the spin-incoherent Bose gas has a broadened momentum

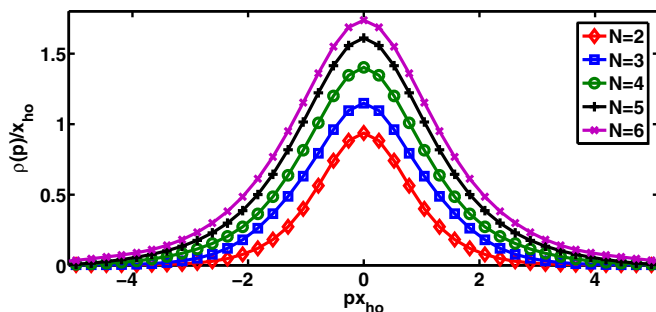


FIG. 1. Momentum distributions of a spin-incoherent 1D spin-1 TG gas up to $N = 6$ in the sector of $S_z = 0$. Uniformly broadened distributions as N grows are demonstrated, which are due to the spin function overlaps.

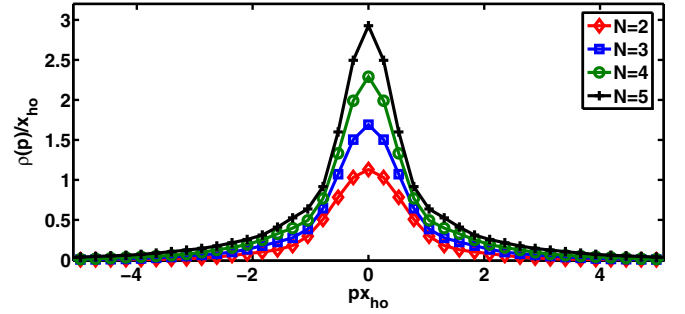


FIG. 2. Momentum distributions of a 1D spinless TG gas up to $N = 5$. The momentum distributions become sharper as N increases.

distribution relative to the spinless case. Figure 3 shows a direct comparison of spin-1 and spinless cases for $N = 3$ and 5 . At finite temperature, the momentum distribution would also be broadened. However, we shall see below that these two situations can be easily distinguished.

In Figs. 4 and 5, we show the large momentum asymptotics in logarithmic scales and compare with our analytic calculations in Sec. IV. The asymptotics for the spinless case can be obtained from Eq. (29) by replacing $(1 + w_{2N}/w_N)$ by 2. The $N = 2$ case can also be evaluated exactly [45]. Our numerical results match well with the exact ones for $px_{ho} \lesssim 4$. Moreover, we see that although the momentum distributions by MC integration are approaching their asymptotic values for increasing p , the differences between them remain rather large (around a factor of 3) for $px_{ho} \approx 4$. For even larger momentum $p \gtrsim 6$, the differences become larger because of the inaccuracy of MC integration. For larger N , one may expect that the asymptotics would take even larger p to reach [14]. Our numerical results become inaccurate for large p for larger N 's. However, we can still make use of the asymptotics to improve our evaluation of the total kinetic energy of the system, as discussed below. For the spinless case, we also show the results from the asymptotic formula $\approx 0.1297 \times N^{3/2}/\bar{k}^4$ proposed by Olshanii and Dunjko [14]. We see that in Fig. 5, for $N = 5$, this value is much below the asymptotic that we obtain from (the modified) Eq. (29).

At finite temperature, we show in Fig. 6 that the momentum distributions are broadened as the temperature increases. The spinless case always has higher peaks than the spin-1 bosons

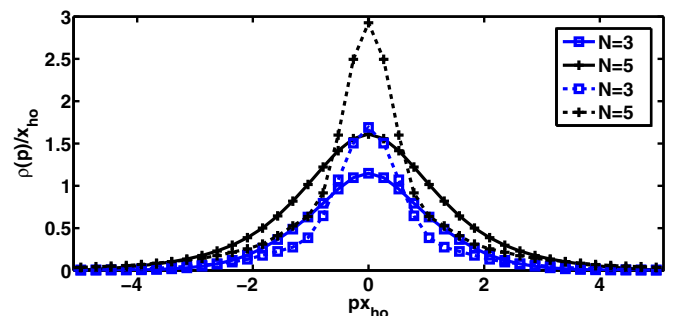


FIG. 3. Comparison of the momentum distributions of spin-incoherent 1D spin-1 (solid) and 1D spinless (dash) TG gases for $N = 3$ and 5 .

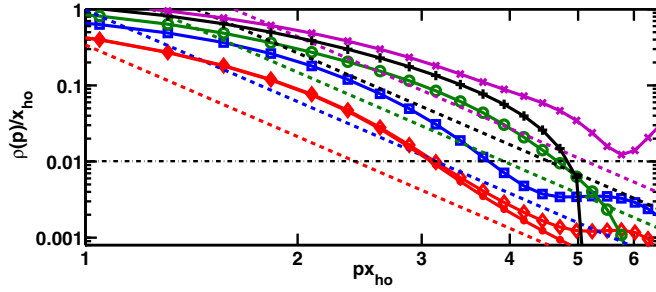


FIG. 4. Asymptotics of large momentum distributions in Fig. 1. Large momentum asymptotics are plotted in logarithmic scales and compared with analytic calculations (dash) in a 1D spin-1 TG gas. (a) The analytically derived asymptotics are $0.34/p^4$, $0.98/p^4$, $2.38/p^4$, $4.27/p^4$, and $6.98/p^4$ respectively for $N = 2-6$. The result of $N = 2$ (dash- \bullet) obtained by conventional numerical integration almost overlaps with the one by Monte Carlo integration, which asymptotically approaches the analytic curve in large p limit as expected. The line symbols and colors follow Fig. 1, and a horizontal line of 10^{-2} is used to guide the eye for approximately the accuracy for the Monte Carlo results.

at the same temperature. The case of $N = 3$ is numerically averaged over all orbitals by $e^{-\beta E_s}$ [$\beta \equiv 1/(k_B T)$] at the cutoff of $E_s = 6\hbar\omega$ where it shows no significant changes when including more orbitals. We also compare the spin-1 bosons at zero temperature with the spinless case at $T = 0.65\hbar\omega/k_B$ where they almost overlap at the peaks while differing in the tails of the momentum distributions as shown in the inset. The spin-incoherent regime in spin-1 bosons can be distinguished from the spinless ones from the measurements of the momentum distributions and the system energies as well.

The total energy ($\langle E_s \rangle$) of the system is the sum of the potential ($\langle V \rangle$) and kinetic ($\langle K \rangle$) contributions. For our 1D bosonic system in the TG limit, the density distribution is

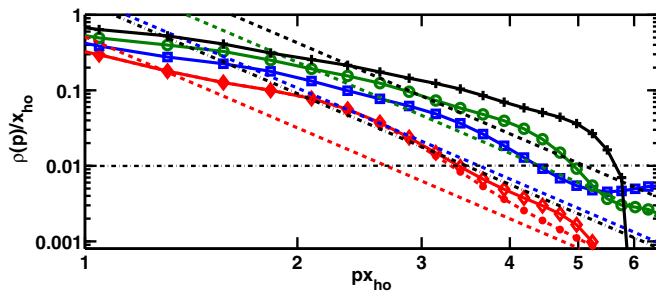


FIG. 5. Asymptotics of large momentum distributions in Fig. 2. Large momentum asymptotics are plotted in logarithmic scales and compared with analytic calculations (dash) in a 1D spinless TG gas. The analytically derived asymptotics are $0.51/p^4$, $1.715/p^4$, $3.77/p^4$, and $6.8/p^4$ respectively for $N = 2-5$, and we also compare with Olshanii's calculation [14] of large momentum result $1.45/p^4$ (dash-dot) for $N = 5$. The result of $N = 2$ (dash- \bullet) obtained by conventional numerical integration again overlaps with the one by Monte Carlo integration, which asymptotically approaches the analytic curve in large p limit as expected. Similarly the line symbols and colors follow Fig. 2, and a horizontal line of 10^{-2} is also plotted for approximately the accuracy for the Monte Carlo results.

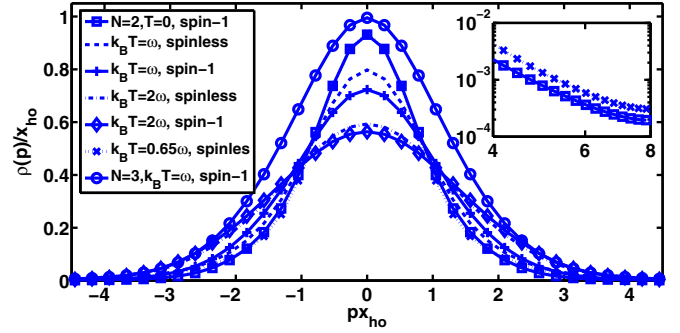


FIG. 6. Momentum distribution comparisons of 1D spin-1 and spinless TG gas at finite temperature. The widths of the distributions broaden as the temperature increases for both the spin-1 and spinless case. To differentiate the momentum distributions of both, a fitting case of spinless bosons at $T = 0.65\hbar\omega/k_B$ (\times) overlaps with spin-1 case at small p , while they differ in the large momentum limit (inset).

identical with a Fermi gas. At zero temperature, we then have $\langle V \rangle = N^2\hbar\omega/4$. The kinetic energy can be obtained easily by considering the action of the Hamiltonian on the wave function at a point where all x_j 's are unequal. We see easily that $\langle K \rangle = N^2\hbar\omega/4$. The above is in accordance with the Virial theorem [46,47], $\langle K \rangle = \langle V \rangle = \langle E_s \rangle/2$. Accordingly, both the momentum distributions in Figs. 1 and 2 have the same value of $\int dp p^2 \rho(p)$. The sharper momentum distribution for the spinless case implies that $\rho(p)$ must be larger at larger p than the spin incoherent case, as can be seen in Fig. 4. Correspondingly, while the momentum distribution of the spinless case broadens with increasing temperature, this broadened distribution is distinct from the broadening due to spin averaging as the total kinetic energy must be higher at finite temperature.

We have also evaluated numerically the potential and kinetic energies by Monte Carlo integration. The potential energy is numerically derived by evaluating $\int dx x^2 \rho(x)$, which is always below the relative error 1.5% to the exact value of $\langle V \rangle$. For $\langle K \rangle \propto \int dp p^2 \rho(p)$, it is more demanding of the accuracy in numerical calculations. We then attach the tails of our momentum distributions by the analytically derived asymptotics starting at around $px_{ho} \approx 4.5$, which improves the relative error of $\langle K \rangle$ significantly to below 9% for example in the case of spin-1 bosons. In Monte Carlo integration of our 1D spin-1 and spinless bosons, the integral boundaries are set to $x = \pm 4x_{ho}$ with 41×41 meshes in $\rho(x, x')$. The results are convergent within $M = 1 \times 10^4$, 1×10^5 , 1×10^6 , 5×10^7 , and 3.5×10^8 for $N = 2-6$, and note that the symmetry of $\rho(x, x') = \rho(x', x)$ can be used to double the M , thus reducing the computation time required for convergence.

VI. CONCLUSION

In conclusion, we have investigated the properties of the spin-incoherent Luttinger liquid in a spin-1 Bose gas. The density matrix of such universal class can be calculated by the spin function overlaps from the highly degenerate spin configurations. We show that the spin function overlap is directly related to the traces of the conjugacy classes in the permutation groups. We also analytically derive the universal

TABLE I. Traces of the conjugacy classes of S_2 .

Traces		
Class	$\text{Tr}_{\chi_1}(G)$	$\text{Tr}_{\chi_2}(G)$
E	1	2
P_{12}	1	0

dependence of $1/p^4$ in large p limit, and compare with the momentum distributions of a spin-1 Bose gas in TG limit using Monte Carlo integrations up to six bosons. The spin-incoherent Bose gas has a broadened momentum distribution which we can confirm and distinguish from the spinless case by measuring its momentum distribution and the total kinetic energy. The ultracold spinor Bose gas thus sets up a promising paradigm to realize this universal while different class of Luttinger liquid.

ACKNOWLEDGMENTS

This work is supported by the Ministry of Science and Technology, Taiwan, under Grants No. MOST-101-2112-M-001-021-MY3 and No. 104-2112-M-001-006-MY3.

APPENDIX: TRACES OF THE CONJUGACY CLASSES OF S_N

Here we list the traces of the conjugacy classes relevant to the spin function overlaps. We note here that the number of conjugacy classes of S_N is 2, 3, 5, 7, and 11 for $N = 2-6$.

For $N = 2$, we have $\{|\chi_1\rangle^P\} = |00\rangle$ and $\{|\chi_2\rangle^P\} = |+-\rangle, |-+\rangle$, respectively. In Table I we have the traces in these bases for E and P_{12} corresponding to two conjugacy classes, and G represents the group operators in relevant conjugacy classes in the calculations of spin function overlaps.

Here $\text{Tr}_{\chi_i}(G) \equiv \sum_{\chi_i} \langle \chi_i | G | \chi_i \rangle$. We note that Tr_χ in the main paper has a relation that $\text{Tr}_\chi = \sum_i \text{Tr}_{\chi_i}$. Since $\{|\chi_2\rangle^P\}$ has two possible number of states, for example of $G = E$, we have $\text{Tr}_\chi(E) = \text{Tr}_{\chi_1}(E) + \text{Tr}_{\chi_2}(E) = 3$.

For $N = 3$, we have $\{|\chi_{1,2}\rangle^P\} = |000\rangle$ and $\{|+-0\rangle^P\}$, respectively, where $\{|+-0\rangle^P\}$ represent six different states by permutations. In Table II we give the traces for the three conjugacy classes, E , P_{12} , and P_{123} , in these sets of states.

For $N = 4$, we have $\{|\chi_{1,2,3}\rangle^P\} = |0000\rangle, \{|+-00\rangle^P\}$, and $\{|+--+ \rangle^P\}$, respectively. In Table III we give the traces for the four conjugacy classes, E , P_{12} , P_{123} , and P_{1234} , in these sets. The other conjugacy class involves $P_{12}P_{34}$ which we do not need in calculating the spin function overlap of Eq. (10) due to the intended order of particle positions we choose in the first place. However, it helps confirm our calculated traces

TABLE II. Traces of the conjugacy classes of S_3 .

Traces		
Class	$\text{Tr}_{\chi_1}(G)$	$\text{Tr}_{\chi_2}(G)$
E	1	6
P_{12}	1	0
P_{123}	1	0

TABLE III. Traces of the conjugacy classes of S_4 .

Traces			
Class	$\text{Tr}_{\chi_1}(G)$	$\text{Tr}_{\chi_2}(G)$	$\text{Tr}_{\chi_3}(G)$
E	1	12	6
P_{12}	1	2	2
P_{123}	1	0	0
P_{1234}	1	0	0

from the identity relation, which we will demonstrate in the end of this Appendix.

For $N = 5$, we have $\{|\chi_{1,2,3}\rangle^P\} = |00000\rangle, \{|+-000\rangle^P\}$, and $\{|+ - + - 0\rangle^P\}$, respectively. In Table IV we give the traces for the five conjugacy classes, E , P_{12} , P_{123} , P_{1234} , and P_{12345} , in these sets.

For $N = 6$, we have $\{|\chi_{1,2,3,4}\rangle^P\} = |000000\rangle, \{|+-0000\rangle^P\}$, $\{|+ - + - 00\rangle^P\}$, and $\{|+ - + - + - \rangle^P\}$, respectively. In Table V we give the traces for the six conjugacy classes, E , P_{12} , P_{123} , P_{1234} , P_{12345} , and P_{123456} , in these sets.

Finally, we demonstrate the details for the construction of conjugacy classes and the calculation of the traces in the class. Take four bosons in the symmetric group S_4 , for example; the classification of the conjugacy classes of S_N can be derived by a cycle decomposition that counts the number of unordered integer partitions. We then decompose four bosons as

$$4, 3 + 1, 2 + 2, 2 + 1 + 1, 1 + 1 + 1 + 1, \rightarrow P_{1234}, P_{123}, P_{12}P_{34}, P_{12}, E, \tag{A1}$$

which accounts for five conjugacy classes. The size of each conjugacy class can be calculated as $N! / [\prod_j (j)^{a_j} a_j!]$ [38], where we have a_j 's integer of j in the unordered integer partitions. This calculation of the size can be also seen as N permutations with a_j times of j 's cycling and a_j permutations of the groups $P_{12\dots j}, P_{j+1\dots 2j}$, etc. Take $\{|\chi_3\rangle^P\}$ of $N = 4$ as an example where we have three classes, E , P_{12} , and $P_{12}P_{34}$, that have nonvanishing traces. Their traces in this basis are 6, 2, and 2 respectively with the sizes 1, 6, and 3. Therefore, the identity relation reads

$$\sum_G \text{Tr}_\chi(G) = 6 \times 1 + 2 \times 6 + 2 \times 3 = 4!, \tag{A2}$$

where the traces are verified.

For the final demonstration of the identity relations in the symmetric group S_5 , the classification of the conjugacy classes

TABLE IV. Traces of some conjugacy classes of S_5 .

Traces			
Class	$\text{Tr}_{\chi_1}(G)$	$\text{Tr}_{\chi_2}(G)$	$\text{Tr}_{\chi_3}(G)$
E	1	20	30
P_{12}	1	6	6
P_{123}	1	2	0
P_{1234}	1	0	0
P_{12345}	1	0	0

TABLE V. Traces of some conjugacy classes of S_6 .

Class	Traces			
	$\text{Tr}_{\chi_1}(G)$	$\text{Tr}_{\chi_2}(G)$	$\text{Tr}_{\chi_3}(G)$	$\text{Tr}_{\chi_4}(G)$
E	1	30	90	20
P_{12}	1	12	18	8
P_{123}	1	6	0	2
P_{1234}	1	2	0	0
P_{12345}	1	0	0	0
P_{123456}	1	0	0	0

becomes

$$\begin{aligned}
& 5, 4 + 1, 3 + 2, 3 + 1 + 1, 2 + 2 + 1, 2 + 1 + 1 + 1, \\
& 1 + 1 + 1 + 1 + 1, \\
& \rightarrow P_{12345}, P_{1234}, P_{123}P_{45}, P_{123}, P_{12}P_{34}, P_{12}, E, \quad (\text{A3})
\end{aligned}$$

which accounts for seven conjugacy classes. We can verify the traces of each conjugacy class by the identity relation. Take $\{|\chi_2\}^P$ of $N = 5$ as an example,

$$\sum_G \text{Tr}_\chi(G) = 20 \times 1 + 6 \times 10 + 2 \times 20 = 5!, \quad (\text{A4})$$

where the sizes of P_{12} and P_{123} are 10 and 20, respectively. Lastly, for $\{|\chi_3\}^P$, we have

$$\sum_G \text{Tr}_\chi(G) = 30 \times 1 + 6 \times 10 + 2 \times 15 = 5!, \quad (\text{A5})$$

where the size of 15 belongs to $P_{12}P_{34}$ and its trace is 2. The above examples show the identity relation between the total traces of the conjugacy classes and the order of S_N .

-
- [1] T. Giamarchi, *Quantum Physics in One Dimension* (Oxford University Press, Oxford, 2004).
- [2] F. D. M. Haldane, *Phys. Rev. Lett.* **47**, 1840 (1981); *J. Phys. C: Solid State Phys.* **14**, 2585 (1981).
- [3] G. A. Fiete, *Rev. Mod. Phys.* **79**, 801 (2007).
- [4] M. A. Cazalilla, R. Citro, T. Giamarchi, E. Orignac, and M. Rigol, *Rev. Mod. Phys.* **83**, 1405 (2011).
- [5] T. L. Ho, *Phys. Rev. Lett.* **81**, 742 (1998).
- [6] B. Paredes, A. Widera, V. Murg, O. Mandel, S. Föling, I. Cirac, G. V. Shlyapnikov, and T. W. Hänsch, and I. Bloch, *Nature (London)* **429**, 277 (2004).
- [7] T. Kinoshita, T. Wenger, and D. S. Weiss, *Science* **305**, 1125 (2004).
- [8] E. Haller, M. Gustavsson, M. J. Mark, J. G. Danzl, R. Hart, G. Pupillo, and H.-C. Nägerl, *Science* **325**, 1224 (2009).
- [9] L. Tonks, *Phys. Rev.* **50**, 955 (1936).
- [10] M. D. Girardeau, *J. Math. Phys.* **1**, 516 (1960).
- [11] M. D. Girardeau, E. M. Wright, and J. M. Triscari, *Phys. Rev. A* **63**, 033601 (2001).
- [12] M. D. Girardeau and A. Minguzzi, *Phys. Rev. Lett.* **99**, 230402 (2007).
- [13] A. Minguzzi, P. Vignolo, and M. P. Tosi, *Phys. Lett. A* **294**, 222 (2002).
- [14] M. Olshanii and V. Dunjko, *Phys. Rev. Lett.* **91**, 090401 (2003).
- [15] W. Xu and M. Rigol, *Phys. Rev. A* **92**, 063623 (2015).
- [16] F. Deuretzbacher, K. Fredenhagen, D. Becker, K. Bongs, K. Sengstock, and D. Pfannkuche, *Phys. Rev. Lett.* **100**, 160405 (2008).
- [17] F. Deuretzbacher, D. Becker, J. Bjerlin, S. M. Reimann, and L. Santos, *Phys. Rev. A* **90**, 013611 (2014).
- [18] A. G. Volosniev, D. V. Fedorov, A. S. Jensen, M. Valiente, and N. T. Zinner, *Nat. Commun.* **5**, 5300 (2014).
- [19] L. Yang, L. Guan, and H. Pu, *Phys. Rev. A* **91**, 043634 (2015).
- [20] F. Deuretzbacher, D. Becker, and L. Santos, *Phys. Rev. A* **94**, 023606 (2016).
- [21] N. L. Harshman, *Phys. Rev. A* **89**, 033633 (2014).
- [22] V. A. Yurovsky, *Phys. Rev. Lett.* **113**, 200406 (2014).
- [23] I. Shvachuck, Ch. Buggle, D. S. Petrov, K. Dieckmann, M. Zielonkowski, M. Kemmann, T. G. Tiecke, W. von Klitzing, G. V. Shlyapnikov, and J. T. M. Walraven, *Phys. Rev. Lett.* **89**, 270404 (2002).
- [24] M. J. Davis, P. B. Blakie, A. H. van Amerongen, N. J. van Druten, and K. V. Kheruntsyan, *Phys. Rev. A* **85**, 031604 (2012).
- [25] T. Jacqmin, B. Fang, T. Berrada, T. Roscilde, and I. Bouchoule, *Phys. Rev. A* **86**, 043626 (2012).
- [26] B. Fang, A. Johnson, T. Roscilde, and I. Bouchoule, *Phys. Rev. Lett.* **116**, 050402 (2016).
- [27] M. Kozuma, L. Deng, E. W. Hagley, J. Wen, R. Lutwak, K. Helmerson, S. L. Rolston, and W. D. Phillips, *Phys. Rev. Lett.* **82**, 871 (1999).
- [28] J. Stenger, S. Inouye, A. P. Chikkatur, D. M. Stamper-Kurn, D. E. Pritchard, and W. Ketterle, *Phys. Rev. Lett.* **82**, 4569 (1999).
- [29] J. Steinhauer, R. Ozeri, N. Katz, and N. Davidson, *Phys. Rev. Lett.* **88**, 120407 (2002).
- [30] S. B. Papp, J. M. Pino, R. J. Wild, S. Ronen, C. E. Wieman, D. S. Jin, and E. A. Cornell, *Phys. Rev. Lett.* **101**, 135301 (2008).
- [31] G. Veeravalli, E. Kuhnle, P. Dyke, and C. J. Vale, *Phys. Rev. Lett.* **101**, 250403 (2008).
- [32] J. M. Pino, R. J. Wild, P. Makotyn, D. S. Jin, and E. A. Cornell, *Phys. Rev. A* **83**, 033615 (2011).
- [33] V. V. Cheianov, H. Smith, and M. B. Zvonarev, *Phys. Rev. A* **71**, 033610 (2005).
- [34] T. Ohmi and K. Machida, *J. Phys. Soc. Jpn.* **67**, 1822 (1998).
- [35] M. Olshanii, *Phys. Rev. Lett.* **81**, 938 (1998).
- [36] V. A. Yurovsky, M. Olshanii, and D. S. Weiss, *Adv. At. Mol. Opt. Phys.* **55**, 61 (2008).
- [37] D. M. Stamper-Kurn and M. Ueda, *Rev. Mod. Phys.* **85**, 1191 (2013).
- [38] M. Hamermesh, *Group Theory and Its Application to Physical Problems* (Dover Publications, New York, 1989).
- [39] S. Tan, *Ann. Phys. (NY)* **323**, 2952 (2008).
- [40] E. Braaten and L. Platter, *Phys. Rev. Lett.* **100**, 205301 (2008).
- [41] E. Braaten, D. Kang, and L. Platter, *Phys. Rev. A* **78**, 053606 (2008).
- [42] F. Werner, L. Tarruell, and Y. Castin, *Eur. Phys. J. B* **68**, 401 (2009).
- [43] S. Zhang and A. J. Leggett, *Phys. Rev. A* **79**, 023601 (2009).
- [44] M. Barth and W. Zwerger, *Ann. Phys. (NY)* **326**, 2544 (2011).
- [45] The result of $N = 2$ can be obtained by conventional numerical integration. Using Eqs. (3) and (15), and same manipulation

below Eq. (15), we have

$$\begin{aligned} \rho(x < x')/2 &= \phi_0(x)\phi_0(x') + \phi_1(x)\phi_1(x) \\ &\quad - \frac{4}{3} \int_x^{x'} dx_2 [\phi_0(x)\phi_1(x_2) - \phi_1(x)\phi_0(x_2)] \\ &\quad \times [\phi_0(x')\phi_1(x_2) - \phi_1(x')\phi_0(x_2)], \end{aligned}$$

where the factor $(-4/3)$ is due to the averaged spin function overlap $(1/3)$ for a spin-1 Bose gas. The above also applies to the cases of a noninteracting fermions or spinless bosons when we let $(-4/3 \rightarrow 0)$ or $(-4/3 \rightarrow -2)$, respectively.

[46] F. Werner and Y. Castin, *Phys. Rev. A* **74**, 053604 (2006).

[47] F. Werner, *Phys. Rev. A* **78**, 025601 (2008).